

Simulation of the Ising Model using the Monte Carlo Method on Different Types of Lattices

Ortiz Jose

University of Antioquia (UdeA)

Abstract

A numerical implementation of the Ising model is presented using the Monte Carlo method with Metropolis dynamics, analyzing the behavior of magnetization (m) and energy in different types of lattices (linear, square, honeycomb, and cubic) exposed to a temperature reservoir (T) and an external magnetic field (H), both in the paramagnetic and ferromagnetic regimes. The influence of T and occupancy (ratio between occupied and available sites in the Ising lattices) on phase transitions and the system's magnetic response to H is also studied. It is concluded that in the paramagnetic case, increasing T makes it more difficult to vary m in the system due to the induced disorder. For the paramagnetic case, it is found that m follows a $\tanh(x)$ law with respect to the ratio H and T . It is concluded that in the ferromagnetic case, hysteresis cycles exist, showing a "memory" of the system, in addition to a dependence on the "number of neighbors" (z) of the lattices. Finally, m is varied as a function of T , and it is found that there are different critical temperatures T_c at which the systems change phase and that these depend proportionally on z (for these systems).

1 Introduction

The study of magnetization phenomena, such as ferromagnetism, paramagnetism, diamagnetism, among others, has enabled the development of technologies necessary for societal progress, such as electric motors, generators, hard drives, nuclear magnetic resonance, etc. [1] To develop a theory that could serve as a basis for explaining these phenomena, the Ising model was born, one that is still used today in systems modeled (a priori) as a set of molecules whose interactions between the elements that compose them are due (in part) to the presence of nearest neighbors. [2]

In 1920, the German physicist Wilhelm Lenz proposed a model as a simplification to explain the behavior of ferromagnetic magnets. Lenz suggested a system of spins arranged on a lattice; in this system, each spin would interact with its nearest neighbors, tending to align in the same direction as them. This system was assigned to his doctoral student, Ernst Ising, who in his 1924 thesis analyzed the model in one dimension. Although the linear lattice that Ising initially assumed to explain the phenomenon did not yield satisfactory results, other lattices studied later proved useful. [3]

The Ising model works by representing atoms or spins on a lattice (such as a 1D, 2D, or 3D grid) where each spin can point up or down. The total energy of the system is calculated considering interactions between neighboring spins and a possible external magnetic field. Using the Boltzmann distribution, the collective behavior can be predicted and information extracted, such as phase transitions. This model is fundamental, as it serves as a basis for more complex extensions like the Potts model, the XY model, or the Heisenberg model, which study phenomena in condensed matter physics,

biology, and computation. Its simplicity allows exact solutions in low dimensions and numerical simulations in real problems. [4]

Currently, this model has evolved by attempting to incorporate new degrees of freedom, such as lattice structure, multicomponent spins, long-range interactions, and quantum perturbations. Research is focusing on combinatorial optimization and biological data analysis. "Ising machines" have been developed as low-cost alternatives to conventional quantum computers, mimicking magnetic spins for combinatorial optimization [5–8]. However, significant problems persist that limit the scope of the Ising model. One of the most well-known problems is the absence of an exact solution for the model in three (or more) dimensions, which prevents a complete analytical understanding of transition phenomena. Additionally, in the field of Ising machines, practical limitations are faced due to high energy consumption and possible lack of scalability [9, 10].

Computational methods, such as Monte Carlo (MC) simulations, play a crucial role in the Ising model by solving problems that lack analytical solutions, especially for dimensions greater than 2. These generate random spin configurations according to the Boltzmann distribution, using algorithms like Metropolis to obtain statistical averages and thus extract thermodynamic properties such as magnetization or critical temperature [11–13].

In this work, MC simulations with Metropolis dynamics will be implemented for the Ising model on different lattices, with different occupancies using periodic boundary conditions. For the paramagnetic case, magnetization curves m vs H will be obtained. For three isotherms, the equation of state law m vs H/T will be verified by fitting to a particular structure with $\tanh(x)$. For the ferromagnetic case, isotherms will be simulated to observe the hysteresis cycle. Finally, isotherms m

vs H will be simulated and it will be discussed how variations in temperature as a function of occupancies and imposed lattices influence.

2 Theoretical Framework

In the Ising model, a set of N spins located at the sites of a lattice is considered. Each i -th spin s_i can adopt one of two discrete states ± 1 . These states represent the intrinsic atomic magnetic moments in a material [14].

The Hamiltonian \mathcal{H} of the system, in its canonical form, is expressed as:

$$\mathcal{H}(\{s_i\}) = -J \sum_{\langle i,j \rangle} s_i s_j - H \sum_{i=1}^N s_i, \quad (1)$$

where:

- $\{s_i\}$ denotes a specific configuration of all the spins.
- J is the exchange coupling constant, which quantifies the strength of the interaction between adjacent spins.
- The sum $\sum_{\langle i,j \rangle}$ extends over all pairs of nearest-neighbor spins on the lattice. The symbol $\langle i, j \rangle$ indicates that only local interactions are considered.
- H represents the strength of a uniform external magnetic field applied to the system.

This formulation will work with the Boltzmann constant $k_B = 1$, simplifying subsequent thermodynamic expressions.

With this definition, a fundamental relationship in statistical mechanics can be established, which is between the Hamiltonian and the partition function Z , defined by

$$Z = \sum_{\{S_i\}} e^{-\beta H(\{S_i\})} \quad (2)$$

where $\beta = 1/(k_B T)$, and the sum extends over all 2^N possible spin configurations. This partition function is key to deriving thermodynamic properties: the Helmholtz free energy is obtained from it as

$$F = -\frac{1}{\beta} \ln Z, \quad (3)$$

the internal energy as

$$E = -\frac{\partial \ln Z}{\partial \beta}, \quad (4)$$

and the magnetization as

$$m = \frac{1}{\beta N} \frac{\partial \ln Z}{\partial H}. \quad (5)$$

Clearly, in the thermodynamic limit ($N \rightarrow \infty$), these quantities provide the macroscopic behavior of the system, allowing analytical and/or numerical study of phases and critical transitions.

In the framework of the Ising model, the paramagnetic and ferromagnetic phases represent two fundamental thermodynamic regimes that arise from spin interactions, which depend on the temperature T , the external magnetic field H , and the coupling constant J .

2.1 Paramagnetism and Ferromagnetism in Ising

Paramagnetism manifests in systems where spin interactions are negligible ($J = 0$), reducing the Hamiltonian to

$$\mathcal{H} = -H \sum_i s_i. \quad (6)$$

In this case, each spin behaves independently, responding only to the external field H and the thermal disorder induced by T . In fact, by eliminating the interaction term ($J = 0$), the energy of each spin is simply $-H s_i$, implying that the spins do not feel the nearest neighbors.

The partition function for an isolated spin is

$$Z = 2 \cosh(\beta H), \quad (7)$$

where $\beta = 1/(k_B T)$. Thus, for N independent spins,

$$Z = [2 \cosh(\beta H)]^N. \quad (8)$$

For the ferromagnetic case ($J > 0$), interactions favor collective alignment of spins even in the absence of an external field ($H = 0$). At low temperatures ($T < T_c$), the system exhibits spontaneous magnetization, while otherwise m disappears. This smooth discontinuity in $m(T)$ characterizes the ferromagnetic phase transition of the system.

2.2 Example and Analysis: 1D and 2D Cases

2.2.1 One-Dimensional Case (1D)

Consider the 1D Ising chain with coupling $J > 0$ and external field $H = 0$ (periodic boundary conditions). Using the transfer matrix technique, the partition function and free energy per spin are obtained. With $k_B = 1$,

$$Z_N = \lambda_+^N + \lambda_-^N, \quad (9)$$

where λ_{\pm} are the eigenvalues of the transfer matrix. For $H = 0$, this expression simplifies and the free energy per spin in the thermodynamic limit $N \rightarrow \infty$ is

$$f = -\frac{1}{\beta} \ln (2 \cosh(\beta J)). \quad (10)$$

From this, the magnetization per spin at $H = 0$ is deduced as

$$m(T) = 0 \quad (\forall T > 0), \quad (11)$$

that is, there is no spontaneous magnetization and thus no phase transition at finite temperature in one dimension. The correlation length ξ is given by

$$\xi^{-1} = -\ln (\tanh(\beta J)), \quad (12)$$

which diverges only in the limit $T \rightarrow 0$ (as expected).

2.2.2 Two-Dimensional Case (2D)

In two dimensions, the Ising model on a square lattice was solved by Onsager (partition function) and Yang (magnetization). The main conclusion is that there is a phase transition at a finite critical temperature T_c . With $k_B = 1$, the critical temperature is

$$T_c = \frac{2J}{\ln(1 + \sqrt{2})}. \quad (13)$$

For $T < T_c$, the magnetization per spin at $H = 0$ (Yang's result) is given by

$$m(T) = \left[1 - \sinh^{-4}(2\beta J)\right]^{1/8}, \quad (T < T_c), \quad (14)$$

and $m(T) = 0$ for $T \geq T_c$. The free energy per spin (Onsager's result) has a closed but more complex expression; its explicit form can be found in the classical literature on the subject. These results demonstrate that, unlike the 1D case, in 2D the model exhibits a second-order phase transition with non-trivial critical exponents. [15–17]

2.3 Monte Carlo Method and Metropolis Dynamics

Given that the configuration space of the Ising model grows exponentially with the number of spins, exact evaluation of the system's thermodynamic properties is infeasible for large systems. Therefore, numerical methods such as Monte Carlo methods [18] must be employed, which allow efficient exploration of the microstate space.

Instead of calculating exactly, the process is simulated many times with random numbers and the results are averaged. The more simulations, the more accurate the approximation (due to the law of large numbers).

Within Monte Carlo methods, the Metropolis algorithm is a specific variant within Markov chain Monte Carlo (MCMC) techniques. Its goal is to sample a complex probability distribution efficiently when direct sampling is not possible.

The Metropolis process starts from an initial state and proposes random moves to new system states. For each proposal, the probability ratio between the new state and the current state is calculated; the acceptance probability in this case is

$$P_{\text{accept}} = \min\{1, e^{-\beta\Delta\mathcal{H}}\}, \quad (15)$$

where $\Delta\mathcal{H} = \mathcal{H}_{\text{new}} - \mathcal{H}_{\text{current}}$. If the proposal is more favorable (higher probability), it is accepted; otherwise, it is accepted with the aforementioned probability, and if not accepted, the system remains in the current state. This method is effective because it guides samples toward high-probability regions, making it very useful for estimating thermodynamic averages and numerically studying phase transitions.

2.4 Computational Methodology and Monte Carlo Simulations for the Ising Model

The implementation of Monte Carlo (MC) simulations with Metropolis dynamics will be carried out in `Python`, using multidimensional arrays. Modules for visualization and optimization will be employed due to the high computational demand required to perform multiple simulations.

Linear, square, hexagonal, and cubic lattice systems will be implemented, with coordination numbers (number of neighbors) $z = 2$, $z = 4$, $z = 3$, and $z = 8$,

respectively. The magnetic field will be varied and the evolution of the system characteristics will be observed, all for three isotherms.

The variation of magnetization in terms of the magnetic field will be analyzed, as well as how it changes as a function of $\frac{H}{T}$, and it will be compared with the analytical solution, which has the form $\tanh(x)$ (for those cases where an analytical solution exists).

The calculations will start with a number of possible locations within a lattice of size `SIZE` = 100. If the lattice is expected to have symmetric sides, then the dimensions for the different lattices, in terms of this `SIZE`, will be as follows:

- **Linear chain:** For this case, $L = 100$, since each position is uniformly distributed along a one-dimensional line.
- **Hexagonal lattice (honeycomb):** In this case, the lattice is of size $L \times L$ but with a bipartite structure; that is, it can be understood as two sublattices per unit cell, which allows defining their neighbors. Clearly, `SIZE` = L , with $N = 2L^2$.
- **Square lattice:** In this case, `SIZE` = L , with $N = L^2$.
- **Cubic lattice:** The total size is L^3 , with two sites per cell. If `SIZE` = L , then $N = 2L^3$.

The code flow can be carried out considering different sections.

2.4.1 Lattice Definition

An array is proposed that represents all possible sites of the lattice. Depending on this lattice, the possible neighbors that it can have will be defined. Upon completing the dilution value q , the number of elements occupying the lattice will be obtained.

2.4.2 Neighbors

For the different topologies, specific neighbors will be defined. For all lattices, periodic boundary conditions are assumed. This is for the situation in which the neighbors of the elements located on the boundaries of the systems will be evaluated or worked with.

For the one-dimensional linear lattice, it is proposed that each element of the lattice has a neighbor to the left and one to the right. For a two-dimensional square lattice, the neighbors are naturally defined as up, down, left, and right.

A different case is the honeycomb-type lattice. It can be assumed as two interpenetrating sublattices, A and B. Each site of one sublattice interacts exclusively with three neighbors of the opposite sublattice, reflecting a hexagonal geometry. This, in turn, is assumed in two dimensions.

Finally, a three-dimensional cubic lattice will be assumed. Analogously to the honeycomb-type lattice, two interpenetrating sublattices are organized: one formed by the vertices of the cubic cell and the other by the centers of each cube. Each site has eight contiguous neighbors located at the vertices of the surrounding cube, all belonging to the complementary sublattice. That is, a three-dimensional bipartite structure.

2.4.3 Thermalization

In this section, the system is stabilized to perform measurements.

It starts from a random configuration, that is, the system is initialized with spins distributed randomly, depending on an occupancy number $q = n/N$, where n is the number of spins in the system, which does not represent the thermal equilibrium state at a given temperature.

Then, many MC steps are performed, that is, the system is allowed to evolve as a "real" system, in which, at a given instant of time, a random spin spontaneously changes its state (i.e., flips). Then, it is decided whether to allow this spin to flip or not; this, based on the selection rule presented in [2.3]. In this way, the system is allowed to evolve, forgetting the initial conditions and creating a very probable configuration based on the given temperature.

2.4.4 Sampling

The system continues to evolve in the same way as thermalization; the change is that now the values are recorded. Every certain number of steps, the value of the magnetization (or energy) of the system at that instant is recorded. After enough samples have been accumulated, they are averaged. However, since no preference can be given to the initial assumption in thermalization, what is done is to assume multiple configurations and calculate the average value of the magnetization; this will be the value of the magnetization or energy for a given value of the magnetic field.

In the case of calculating the values with respect to H/T , it is done similarly to the previous steps. It is clear that it is indifferent to start with a particular configuration, since it does not contain preference; that is, one could have chosen it in such a way that all spins were aligned and it would have been the same.

3 Results

For a paramagnetic case ($J = 0$), the following graphs of the variation of magnetization as a function of the induced magnetic field were obtained

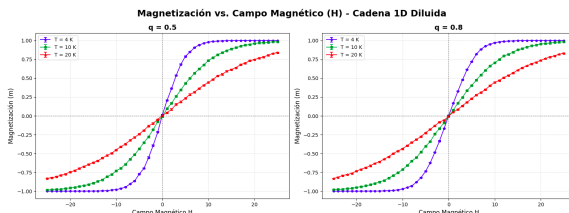


Figure 1. Behavior of magnetization for the paramagnetic case ($J = 0$) of a linear lattice.

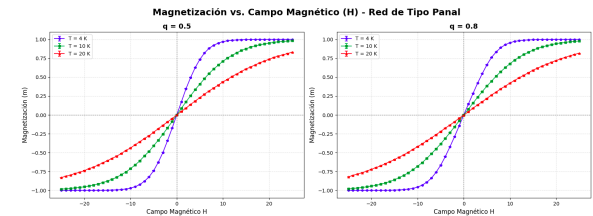


Figure 2. Behavior of magnetization for the paramagnetic case ($J = 0$) of a honeycomb-type lattice.

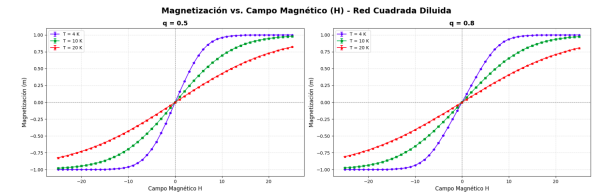


Figure 3. Behavior of magnetization for the paramagnetic case ($J = 0$) of a square-type lattice.

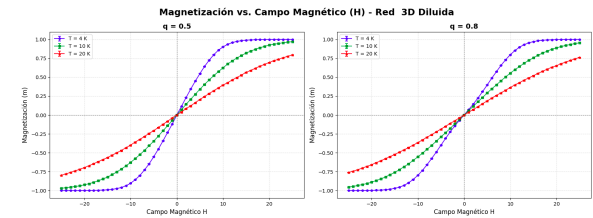


Figure 4. Behavior of magnetization for the paramagnetic case ($J = 0$) of a cubic-type lattice.

Clearly, there is a symmetric dependence with respect to the applied field, consistent with the absence of interactions between spins. Likewise, temperature directly influences the slope of the $m(H)$ curves, as higher temperature reduces the magnetic response due to increased thermal disorder, which decreases the alignment of spins in the applied field. This behavior is consistent with Curie's law, according to which the magnetic susceptibility of a paramagnetic material varies inversely with temperature.

On the other hand, the internal energy E of the system can be analyzed as a function of the number of Monte Carlo steps. For this, it is appropriate to consider some values of H and take the different values of E at certain moments of the process.

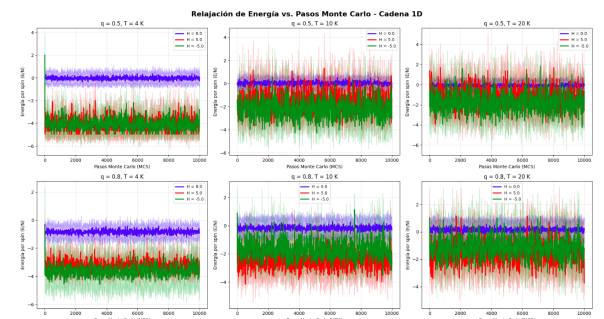


Figure 5. Relaxation of the system ($J = 0$) of a linear-type lattice.

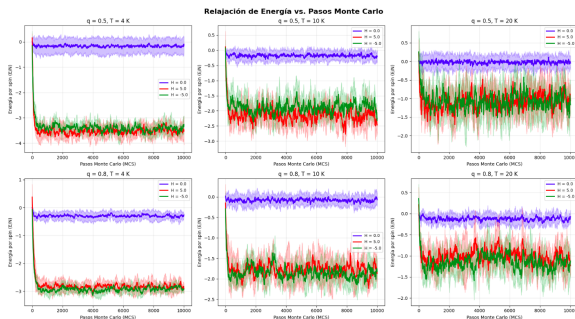


Figure 6. Relaxation of the system ($J = 0$) of a honeycomb-type lattice.

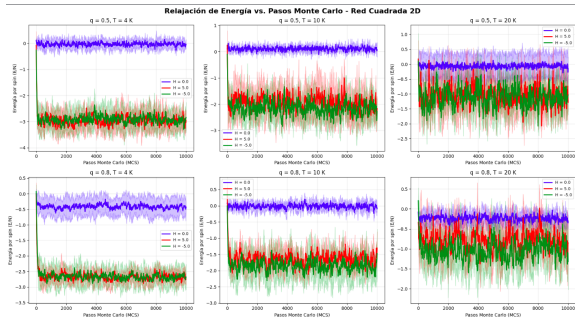


Figure 7. Relaxation of the system ($J = 0$) of a square-type lattice.

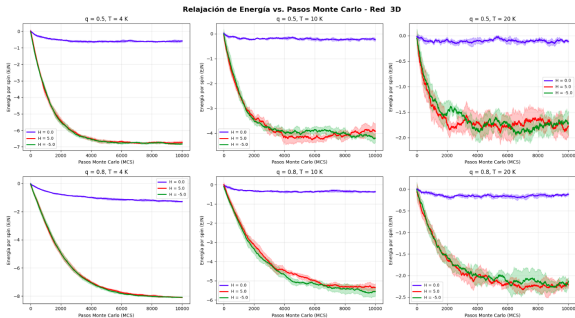


Figure 8. Relaxation of the system ($J = 0$) of a cubic-type lattice.

In all graphs, it is observed that the energy values tend to stabilize as the number of iterations increases, which makes sense, as an equilibrium point is always reached where the system reaches a stable state with a reservoir that is assumed to be transferring heat to it.

On the other hand, the behavior of the graphs of m vs H/T can be visualized.

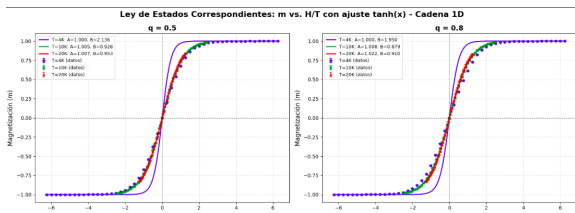


Figure 9. Equation of state ($J = 0$) of a linear-type lattice.

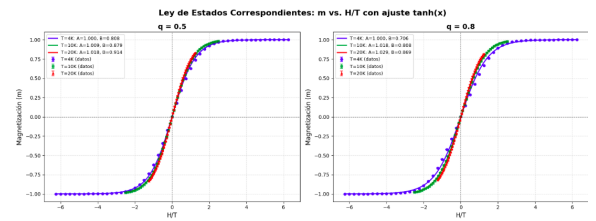


Figure 10. Equation of state ($J = 0$) of a honeycomb-type lattice.

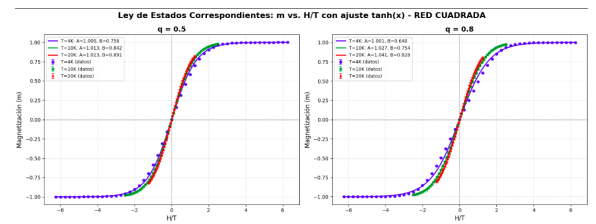


Figure 11. Equation of state ($J = 0$) of a square-type lattice.

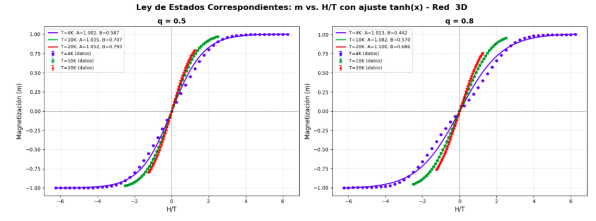


Figure 12. Equation of state ($J = 0$) of a cubic-type lattice.

In the paramagnetic regime ($J = 0$), the spins behave independently, so the coordination number z does not influence the result. All lattices present the same magnetization curves $m(H)$ with symmetric shape, which saturate at ± 1 and fit perfectly to the law $m = \tanh(H/T)$, as well as equivalent energy relaxation processes.

In contrast, the magnetic dilution q does have an effect: it linearly reduces the amplitude of the magnetization according to $m = q \tanh(H/T)$. For $q = 0$, there is no magnetization or energy variation; for $q = 0.5$ and $q = 0.8$, the curves maintain the same shape but with proportional saturations and faster thermalization due to fewer active spins. Overall, the results confirm that in the absence of interactions, the magnetic response depends only on H , T , and q , not on the lattice topology.

However, it is appropriate to analyze the ferromagnetic case, which is based on [2.1]. It can be taken as if the interaction between neighbors were complete. First, it should be noted that the temperature cannot be increased much because in all cases of magnetism, high temperature induces many fluctuations in the system, which prevents observing magnetization even with a strong field. That said, systems in very low temperature regions will be considered. Then, to observe how the system behaves and if it truly has intrinsic magnetization, a cycle can be tested in which the variation of m in terms of H is seen, but now upon reaching maximum saturation, the system is allowed to evolve again with

Monte Carlo but for the same values (in reverse) of H . Thus, the following graphs are obtained.

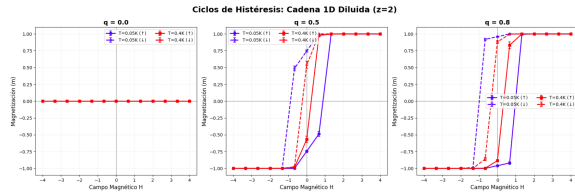


Figure 13. Hysteresis cycle ($J = 1$) of a linear-type lattice.

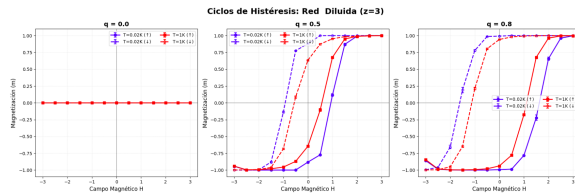


Figure 14. Hysteresis cycle ($J = 1$) of a honeycomb-type lattice.

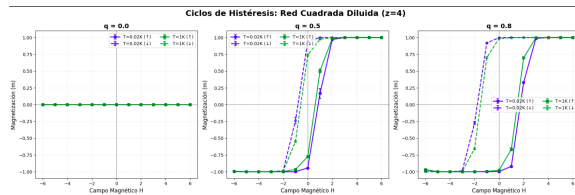


Figure 15. Hysteresis cycle ($J = 1$) of a square-type lattice.

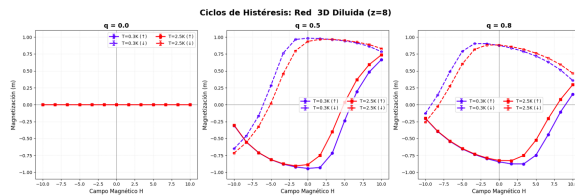


Figure 16. Hysteresis cycle ($J = 1$) of a cubic-type lattice.

It is observed that hysteresis cycles appear when a value $J \neq 0$ is considered, that is, when interactions between spins are included. This generates collective coupling that gives rise to the remnant magnetization characteristic of ferromagnetism.

Additionally, the curves show evident symmetry with respect to the origin, which is consistent with the symmetry of the Hamiltonian under simultaneous inversion of all spins. This invariance implies that

$$m(H) = -m(-H), \quad (16)$$

so the magnetization function is odd in the applied field, as theoretically expected.

Finally, the variation of magnetization as a function of temperature can be analyzed, which allows determining whether there is or not a phase transition in the system.

Additionally, it is possible to simultaneously study other relevant variables, such as the concentration function or the coordination number, to understand how

they influence the collective behavior of the spins and the magnetic response of the system.

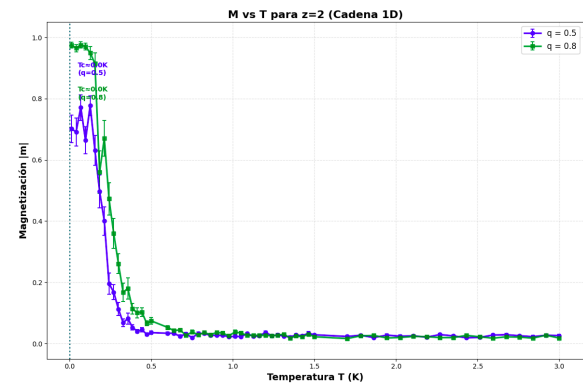


Figure 17. Phase transition ($J = 1$) of a linear-type lattice.

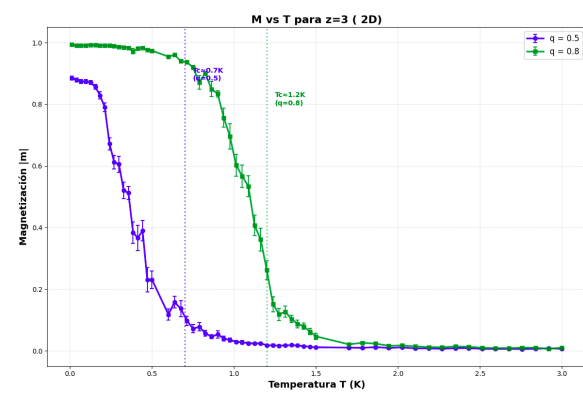


Figure 18. Phase transition ($J = 1$) of a honeycomb-type lattice.

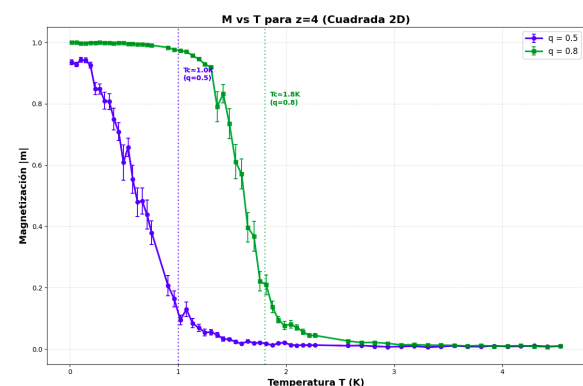


Figure 19. Phase transition ($J = 1$) of a square-type lattice.

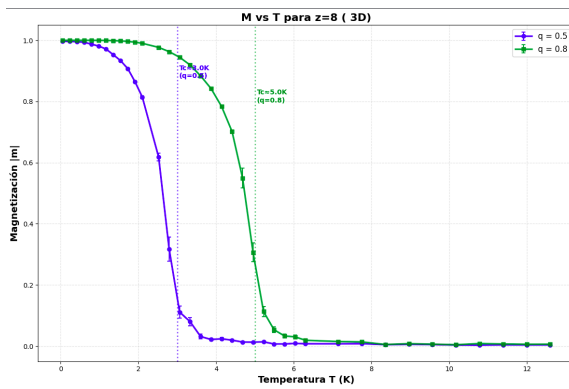


Figure 20. Phase transition ($J = 1$) of a cubic-type lattice.

As can be observed from the graphs, when fixing the dilution and varying and increasing the coordination number, the critical temperature increases. This makes sense, as being linked to more neighbors than others, the intrinsic magnetization will be greater, making it more difficult for them to follow a field going against it or easier if immersed in one in the same direction.

In fact, it makes sense as it follows a rule of

$$T_c \propto zqJ. \quad (17)$$

It should be noted that for the linear case, it is observed that there is no phase transition as it drops abruptly; this is something expected from theory due to section 2. This shows the strengths of these computational methods.

Finally, it can be observed how the system varies at a given moment, in particular what happens at those moments when the temperature increases.

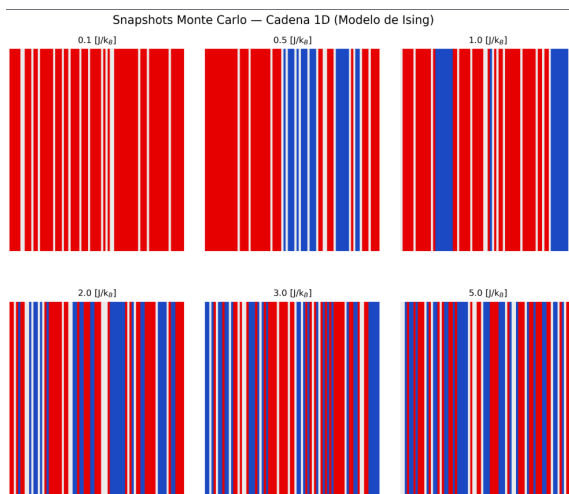


Figure 21. Snapshot ($J = 1$) of a linear-type lattice.

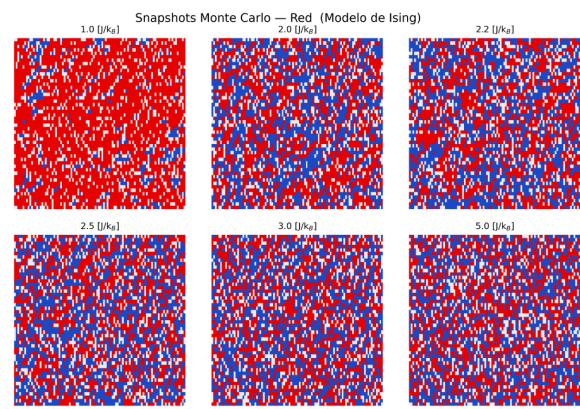


Figure 22. Snapshot ($J = 1$) of a honeycomb-type lattice.

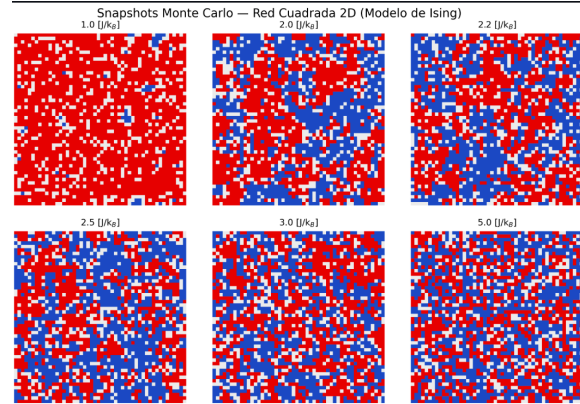


Figure 23. Snapshot ($J = 1$) of a square-type lattice.

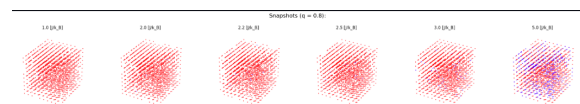


Figure 24. Snapshot ($J = 1$) of a cubic-type lattice.

Clearly, it is noted that as the temperature of the system is increased, the amount of "disorder" or non-alignment of the spins that contribute to the intrinsic magnetization of the system increases. It is clear that all the systems treated previously will present the same characteristics.

4 Conclusions

In this work, the Monte Carlo method with Metropolis dynamics has been implemented to simulate the Ising model on different lattices such as linear, honeycomb, square, and cubic. Considering variations in magnetic dilution q and temperature T , both in paramagnetic and ferromagnetic regimes.

In the paramagnetic case, it is confirmed that the magnetization follows a symmetric dependence on the external magnetic field H , fitting perfectly to the expression $m = q \tanh(H/T)$, regardless of the lattice structure. This highlights the independence of the spins in the absence of interactions, where the topology (coordination

number z) does not play a relevant role. Temperature reduces the magnetic response due to thermal disorder, aligning with Curie's law, while dilution q linearly scales the amplitude of the magnetization and accelerates the thermalization of the system, as evidenced in the energy relaxation curves.

For the ferromagnetic regime, the simulations reveal characteristic hysteresis cycles, with remnant magnetization and odd symmetry $m(H) = -m(-H)$, attributable to collective coupling between spins. These effects are more pronounced at low temperatures, where thermal fluctuations are minimal.

Regarding phase transitions, it is observed that the critical temperature T_c increases with the coordination number z and dilution q , following an approximate relation $T_c \propto zqJ$. In particular, the linear lattice (1D) does not exhibit a phase transition at finite temperature, coinciding with analytical theory, while higher-dimensional lattices show a clear transition from ferromagnetic to paramagnetic, with spontaneous magnetization gradually decreasing to zero as T increases.

The snapshots illustrate how increasing temperature induces greater disorder in spin alignment, reducing intrinsic magnetization in all configurations, underscoring the universal impact of thermal noise on local interactions.

References

- [1] Oliver Gutfleisch, Matthew A. Willard, Ekkes Brück, Christina H. Chen, S. G. Sankar, and J. Ping Liu. Magnetic materials and devices for the 21st century: Stronger, lighter, and more energy efficient. *Advanced Materials*, 23(7):821–842, 2011.
- [2] Stephen G. Brush. History of the lenz-ising model. *Reviews of Modern Physics*, 39(4):883–893, 1967.
- [3] Hugo Duminil-Copin. 100 years of the (critical) ising model on the hypercubic lattice. In *Proceedings of the International Congress of Mathematicians (ICM) 2022, Vol. 1*, page –. EMS Press / International Mathematical Union, 2022. Preliminary version available at arXiv:2208.00864.
- [4] Barry M. McCoy and Jean-Marie Maillard. The importance of the ising model. *Progress of Theoretical Physics*, 127(5):791–817, 2012.
- [5] Hugo Duminil-Copin. Lectures on the ising and potts models on the hypercubic lattice. Technical report, Institut des Hautes Études Scientifiques & Université de Genève, France / Switzerland, 2017. Lecture notes of a class given at the PIMS-CRM Summer School in Probability, June 2017.
- [6] Andrew Lucas. Ising formulations of many np problems. *Frontiers in Physics*, 2:5, 2014. arXiv:1302.5843v3.
- [7] Yoshihisa Yamamoto, Kazuyuki Aihara, Timothée Leleu, Ken ichi Kawarabayashi, Satoshi Kako, Martin Fejer, Kyo Inoue, and Hiroki Takesue. Coherent ising machines—optical neural networks operating at the quantum limit. *npj Quantum Information*, 3(49), 2017.
- [8] Yoshihisa Yamamoto. The future of problem solving: The coherent ising machine approach. *NTT Technical Review*, 20(1):16–19, 2022.
- [9] Farnoosh Khosravi, Mathieu Perreault, Axel Scherer, and Pooya Ronagh. Coherent ising machines: The good, the bad, the ugly. *Preprint*, 2025. Available on ResearchGate and arXiv.
- [10] G. M. Viswanathan. What does it take to solve the 3d ising model? minimal necessary conditions for a valid solution. *Entropy*, 24(11):1665, 2022.
- [11] J. Ostmeyer. The ising model with hybrid monte carlo. *Physics Letters A*, 386:126872, 2021.
- [12] Tianshu Gu. Monte carlo simulation of phase transition in classical ising model. *HSET (Higher School of Engineering Technologies) Journal*, 64(8), 2023.
- [13] Kurt Binder and Erik Luijten. Monte carlo tests of renormalization-group predictions for critical phenomena in ising models (invited review). *Physics Reports*, 344(2-3):179–253, 2001. Invited review on Monte Carlo and critical phenomena.
- [14] Johans Restrepo Cárdenas. *Física Estadística: Teoría, Algoritmos y Problemas*. Profesor del Instituto de Física, Universidad de Antioquia, Medellín, Colombia. Más de 20 años de docencia en Física Estadística.
- [15] Konstantin K. Likharev. 4.5: Modelo ising - resultados exactos y numéricos. In *Posgrado Esencial Física - Mecánica Estadística*. LibreTexts Español, 2024.
- [16] Chen Ning Yang. The spontaneous magnetization of a two-dimensional ising model. *Physical Review*, 85(5):808–816, 1952.
- [17] Raj K. Pathria and Paul D. Beale. *Statistical Mechanics*. Elsevier/Academic Press, 3rd edition, 2011.
- [18] Nicholas Metropolis, Arianna W. Rosenbluth, Marshall N. Rosenbluth, Augusta H. Teller, and Edward Teller. Equation of state calculations by fast computing machines. *The Journal of Chemical Physics*, 21(6):1087–1092, 1953.